bioRxiv preprint doi: https://doi.org/10.1101/091751; this version posted January 9, 2018. The copyright holder for this preprint (which was not certified by peer review) is the author/funder. All rights reserved. No reuse allowed without permission.

Critical transitions and the fragmenting of global forests

Leonardo A. Saravia [1 3], **Santiago R. Doyle** [1], **Ben Bond-Lamberty**[2]

1. Instituto de Ciencias, Universidad Nacional de General Sarmiento, J.M. Gutierrez 1159 (1613), Los Polvorines, Buenos Aires, Argentina.

2. Pacific Northwest National Laboratory, Joint Global Change Research Institute at the University of Maryland–College Park, 5825 University Research Court #3500, College Park, MD 20740, USA

3. Corresponding author e-mail: lsaravia@ungs.edu.ar

keywords: Forest fragmentation, early warning signals, percolation, power-laws, MODIS, critical transitions

Running title: Critical fragmentation in global forest

Abstract

1. Forests provide critical habitat for many species, essential ecosystem services, and are coupled to atmospheric dynamics through exchanges of energy, water and gases. One of the most important changes produced in the biosphere is the replacement of forest areas with human dominated landscapes. This usually leads to fragmentation, altering the sizes of patches, the structure and function of the forest. Here we studied the distribution and dynamics of forest patch sizes at a global level, examining signals of a critical transition from an unfragmented to a fragmented state.

2. We used MODIS vegetation continuous field to estimate the forest patches at a global level and defined wide regions of connected forest across continents and big islands. We search for critical phase transitions, where the system state of the forest changes suddenly at a critical point in time; this implies an abrupt change in connectivity that causes an increased fragmentation level. We combined five criteria to evaluate the closeness of the system to a fragmentation threshold, studying in particular the distribution of forest patch sizes and the dynamics of the largest patch over the last sixteen years.

3. We found some necessary evidence that allows us to analyze fragmentation as a critical transition: all regions followed a power-law distribution over the fifteen years. We also found that the Philippines region probably went through a critical transition from a fragmented to an unfragmented state. Neotropical regions with the highest deforestation rates—South America, Southeast Asia, Africa—all met the criteria to be near a critical fragmentation threshold.

bioRxiv preprint doi: https://doi.org/10.1101/091751; this version posted January 9, 2018. The copyright holder for this preprint (which was not certified by peer review) is the author/funder. All rights reserved. No reuse allowed without permission.

4. This implies that human pressures and climate forcings might trigger undesired effects of fragmentation, such as species loss and degradation of ecosystems services, in these regions. The simple criteria proposed here could be used as an early warning to estimate the distance to a fragmentation threshold in forests around the globe.

bioRxiv preprint doi: https://doi.org/10.1101/091751; this version posted January 9, 2018. The copyright holder for this preprint (which was not certified by peer review) is the author/funder. All rights reserved. No reuse allowed without permission.

Introduction

Forests are one of the most important biomes on earth, providing habitat for a large proportion of species and contributing extensively to global biodiversity (Crowther *et al.*, 2015). In the previous century human activities have influenced global bio-geochemical cycles (Bonan, 2008; Canfield *et al.*, 2010), with one of the most dramatic changes being the replacement of 40% of Earth's formerly biodiverse land areas with landscapes that contain only a few species of crop plants, domestic animals and humans (Foley *et al.*, 2011). These local changes have accumulated over time and now constitute a global forcing (Barnosky *et al.*, 2012). Another global scale forcing that is tied to habitat destruction is fragmentation, which is defined as the division of a continuous habitat into separated portions that are smaller and more isolated. Fragmentation produces multiple interwoven effects: reductions of biodiversity between 13% and 75%, decreasing forest biomass, and changes in nutrient cycling (Haddad *et al.*, 2015). The effects of fragmentation are not only important from an ecological point of view but also that of human activities, as ecosystem services are deeply influenced by the level of landscape fragmentation (Rudel *et al.*, 2005; Angelsen, 2010; Mitchell *et al.*, 2015).

Ecosystems have complex interactions between species and present feedbacks at different levels of organization (Gilman *et al.*, 2010), and external forcings can produce abrupt changes from one state to another, called critical transitions (Scheffer *et al.*, 2009). These abrupt state shifts cannot be linearly forecasted from past changes, and are thus difficult to predict and manage (Scheffer *et al.*, 2009). Such 'critical' transitions have been detected mostly at local scales (Drake & Griffen, 2010; Carpenter *et al.*, 2011), but the accumulation of changes in local communities that overlap geographically can propagate and theoretically cause an abrupt change of the entire system at larger scales (Barnosky *et al.*, 2012). Coupled with the existence of global scale forcings, this implies the possibility that a critical transition could occur at a global scale (Rockstrom *et al.*, 2009; Folke *et al.*, 2011).

Complex systems can experience two general classes of critical transitions (Solé, 2011). In so-called first order transitions, a catastrophic regime shift that is mostly irreversible occurs because of the existence of alternative stable states (Scheffer *et al.*, 2001). This class of transitions is suspected to be present in a variety of ecosystems such as lakes, woodlands, coral reefs (Scheffer *et al.*, 2001), semi-arid grasslands (Bestelmeyer *et al.*, 2011), and fish populations (Vasilakopoulos & Marshall, 2015). They can be the result of positive feedback mechanisms (Villa Martín *et al.*, 2015); for example, fires in some forest ecosystems were more likely to occur in previously burned areas than in unburned places (Kitzberger *et al.*, 2012).

The other class of critical transitions are continuous or second order transitions (Solé & Bascompte, 2006). In these cases, there is a narrow region where the system suddenly changes from one domain to another, with

bioRxiv preprint doi: https://doi.org/10.1101/091751; this version posted January 9, 2018. The copyright holder for this preprint (which was not certified by peer review) is the author/funder. All rights reserved. No reuse allowed without permission.

the change being continuous and in theory reversible. This kind of transitions were suggested to be present in tropical forests (Pueyo *et al.*, 2010), semi-arid mountain ecosystems (McKenzie & Kennedy, 2012), and tundra shrublands (Naito & Cairns, 2015). The transition happens at a critical point where we can observe a distinctive spatial pattern: scale invariant fractal structures characterized by power law patch distributions (Stauffer & Aharony, 1994). There are several processes that can convert a catastrophic transition to a second order transitions (Villa Martín *et al.*, 2015). These include stochasticity, such as demographic fluctuations, spatial heterogeneities, and/or dispersal limitation. All these components are present in forest around the globe (Seidler & Plotkin, 2006; Filotas *et al.*, 2014; Fung *et al.*, 2016), and thus continuous transitions might be more probable than catastrophic transitions. Moreover there is some evidence of recovery in some systems that supposedly suffered an irreversible transition produced by overgrazing (Zhang *et al.*, 2005; Bestelmeyer *et al.*, 2013) and desertification (Allington & Valone, 2010).

The spatial phenomena observed in continuous critical transitions deal with connectivity, a fundamental property of general systems and ecosystems from forests (Ochoa-Quintero *et al.*, 2015) to marine ecosystems (Leibold & Norberg, 2004) and the whole biosphere (Lenton & Williams, 2013). When a system goes from a fragmented to a connected state we say that it percolates (Solé, 2011). Percolation implies that there is a path of connections that involves the whole system. Thus we can characterize two domains or phases: one dominated by short-range interactions where information cannot spread, and another in which long range interactions are possible and information can spread over the whole area. (The term "information" is used in a broad sense and can represent species dispersal or movement.) Thus, there is a critical "percolation threshold" between the two phases, and the system could be driven close to or beyond this point by an external force; climate change and deforestation are the main forces that could be the drivers of such a phase change in contemporary forests (Bonan, 2008; Haddad *et al.*, 2015). There are several applications of this concept in ecology: species' dispersal strategies are influenced by percolation thresholds in three-dimensional forest structure (Solé *et al.*, 2005), and it has been shown that species distributions also have percolation thresholds (He & Hubbell, 2003). This implies that pushing the system below the percolation threshold could produce a biodiversity collapse (Bascompte & Solé, 1996; Solé *et al.*, 2004; Pardini *et al.*, 2010); conversely, being in a connected state (above the threshold) could accelerate the invasion of forest into prairie (Loehle *et al.*, 1996; Naito & Cairns, 2015).

One of the main challenges with systems that can experience critical transitions—of any kind—is that the value of the critical threshold is not known in advance. In addition, because near the critical point a small change can precipitate a state shift of the system, they are difficult to predict. Several methods have been developed to detect if a system is close to the critical point, e.g. a deceleration in recovery from perturbations,

bioRxiv preprint doi: https://doi.org/10.1101/091751; this version posted January 9, 2018. The copyright holder for this preprint (which was not certified by peer review) is the author/funder. All rights reserved. No reuse allowed without permission.

or an increase in variance in the spatial or temporal pattern (Hastings & Wysham, 2010; Carpenter *et al.*, 2011; Boettiger & Hastings, 2012; Dai *et al.*, 2012).

The existence of a critical transition between to states has been established for forest at global scale in different works (Hirota *et al.* (2011); Verbesselt *et al.* (2016); Staal *et al.* (2016); Wuyts *et al.* (2017)). It is generally believed that this constitutes a first order catastrophic transition. The regions where forest can grow are not distributed homogeneously, as there are demographic fluctuations in forest growth and disturbances produced by human activities. Due to new theoretical advances (Villa Martín *et al.*, 2014, 2015) all these factors imply that if these were first order transitions they will be converted or observed as second order continuous transitions. From this basis we applied indices derived from second order transitions to global forest cover dynamics.

In this study, our objective is to look for evidence that forests around the globe are near continuous critical points that represent a fragmentation threshold. We use the framework of percolation to first evaluate if forest patch distribution at a continental scale is described by a power law distribution and then examine the fluctuations of the largest patch. The advantage of using data at a continental scale is that for very large systems the transitions are very sharp (Solé, 2011) and thus much easier to detect than at smaller scales, where noise can mask the signals of the transition.

Methods

Study areas definition

We analyzed mainland forests at a continental scale, covering the whole globe, by delimiting land areas with a near-contiguous forest cover, separated with each other by large non-forested areas. Using this criterion, we delimited the following forest regions. In America, three regions were defined: South America temperate forest (SAT), subtropical and tropical forest up to Mexico (SAST), and USA and Canada forest (NA). Europe and North Asia were treated as one region (EUAS). The rest of the delimited regions were South-east Asia (SEAS), Africa (AF), and Australia (OC). We also included in the analysis islands larger than $10^5 km^2$. The mainland region has the number 1 e.g. OC1, and the nearby islands have consecutive numeration (Appendix S4, figure S1-S6). We applied this criterion to delimit regions because we based our study on percolation theory that assumes some kind of connectivity in the study area (see below).

bioRxiv preprint doi: https://doi.org/10.1101/091751; this version posted January 9, 2018. The copyright holder for this preprint (which was not certified by peer review) is the author/funder. All rights reserved. No reuse allowed without permission.

Forest patch distribution

We studied forest patch distribution in each defined area from 2000 to 2015 using the MODerate-resolution Imaging Spectroradiometer (MODIS) Vegetation Continuous Fields (VCF) Tree Cover dataset version 051 (DiMiceli *et al.*, 2015). This dataset is produced at a global level with a 231-m resolution, from 2000 onwards on an annual basis, the last available year was 2015. There are several definition of forest based on percent tree cover (Sexton *et al.*, 2015); we choose a range from 20% to 40% threshold in 5% increments to convert the percentage tree cover to a binary image of forest and non-forest pixels. This range is centered in the definition used by the United Nations' International Geosphere-Biosphere Programme (Belward, 1996), and studies of global fragmentation (Haddad *et al.*, 2015) and includes the range used in other studies of critical transitions (Xu *et al.*, 2016). Using this range we try to avoid the errors produced by low discrimination of MODIS VCF between forest and dense herbaceous vegetation at low forest cover and the saturation of MODIS VCF in dense forests (Sexton *et al.*, 2013). We repeat all the analysis for this set of thresholds, except in some specific cases described below. Patches of contiguous forest were determined in the binary image by grouping connected forest pixels using a neighborhood of 8 forest units (Moore neighborhood). The MODIS VCF product defines the percentage of tree cover by pixel, but does not discriminate the type of trees so besides natural forest it includes plantations of tree crops like rubber, oil palm, eucalyptus and other managed stands (Hansen *et al.*, 2014).

Percolation theory

A more in-depth introduction to percolation theory can be found elsewhere (Stauffer & Aharony, 1994) and a review from an ecological point of view is available (Oborny *et al.*, 2007). Here, to explain the basic elements of percolation theory we formulate a simple model: we represent our area of interest by a square lattice and each site of the lattice can be occupied—e.g. by forest—with a probability p. The lattice will be more occupied when p is greater, but the sites are randomly distributed. We are interested in the connection between sites, so we define a neighborhood as the eight adjacent sites surrounding any particular site. The sites that are neighbors of other occupied sites define a patch. When there is a patch that connects the lattice from opposite sides, it is said that the system percolates. When p is increased from low values, a percolating patch suddenly appears at some value of p called the critical point p_c.

Thus percolation is characterized by two well defined phases: the unconnected phase when $p < p_c$ (called subcritical in physics), in which species cannot travel far inside the forest, as it is fragmented; in a general sense, information cannot spread. The second is the connected phase when $p > p_c$ (supercritical), species

bioRxiv preprint doi: https://doi.org/10.1101/091751; this version posted January 9, 2018. The copyright holder for this preprint (which was not certified by peer review) is the author/funder. All rights reserved. No reuse allowed without permission.

can move inside a forest patch from side to side of the area (lattice), i.e. information can spread over the whole area. Near the critical point several scaling laws arise: the structure of the patch that spans the area is fractal, the size distribution of the patches is power-law, and other quantities also follow power-law scaling (Stauffer & Aharony, 1994).

The value of the critical point p_c depends on the geometry of the lattice and on the definition of the neighborhood, but other power-law exponents only depend on the lattice dimension. Close to the critical point, the distribution of patch sizes is:

(1) $n_s(p_c) \propto s^{-\alpha}$

where $n_s(p)$ is the number of patches of size s. The exponent α does not depend on the details of the model and it is called universal (Stauffer & Aharony, 1994). These scaling laws can be applied for landscape structures that are approximately random, or at least only correlated over short distances (Gastner *et al.*, 2009). In physics this is called "isotropic percolation universality class", and corresponds to an exponent $\alpha = 2.05495$. If we observe that the patch size distribution has another exponent it will not belong to this universality class and some other mechanism should be invoked to explain it. Percolation thresholds can also be generated by models that have some kind of memory (Hinrichsen, 2000; Ódor, 2004): for example, a patch that has been exploited for many years will recover differently than a recently deforested forest patch. In this case, the system could belong to a different universality class, or in some cases there is no universality, in which case the value of α will depend on the parameters and details of the model (Corrado *et al.*, 2014).

To illustrate these concepts, we conducted simulations with a simple forest model with only two states: forest and non-forest. This type of model is called a "contact process" and was introduced for epidemics (Harris, 1974), but has many applications in ecology (Solé & Bascompte, 2006; Gastner *et al.*, 2009). A site with forest can become extinct with probability e, and produce another forest site in a neighborhood with probability c. We use a neighborhood defined by an isotropic power law probability distribution. We defined a single control parameter as $\lambda = c/e$ and ran simulations for the subcritical fragmentation state $\lambda < \lambda_c$, with $\lambda = 2$, near the critical point for $\lambda = 2.5$, and for the supercritical state with $\lambda = 5$ (see supplementary data, gif animations).

Patch size distributions

We fitted the empirical distribution of forest patches calculated for each of the thresholds on the range we previously mentioned. We used maximum likelihood (Goldstein *et al.*, 2004; Clauset *et al.*, 2009) to fit four distributions: power-law, power-law with exponential cut-off, log-normal, and exponential. We assumed

bioRxiv preprint doi: https://doi.org/10.1101/091751; this version posted January 9, 2018. The copyright holder for this preprint (which was not certified by peer review) is the author/funder. All rights reserved. No reuse allowed without permission.

that the patch size distribution is a continuous variable that was discretized by the remote sensing data acquisition procedure.

We set a minimal patch size (X_{min}) at nine pixels to fit the patch size distributions to avoid artifacts at patch edges due to discretization (Weerman *et al.*, 2012). Besides this hard X_{min} limit we set due to discretization, the power-law distribution needs a lower bound for its scaling behavior. This lower bound is also estimated from the data by maximizing the Kolmogorov-Smirnov (KS) statistic, computed by comparing the empirical and fitted cumulative distribution functions (Clauset *et al.*, 2009). For the log-normal model we constrain the values of the μ parameter to positive values, this parameter controls the mode of the distribution and when is negative most of the probability density of the distribution lies outside the range of the forest patch size data (Limpert *et al.*, 2001).

To select the best model we calculated corrected Akaike Information Criteria (AIC_c) and Akaike weights for each model (Burnham & Anderson, 2002). Akaike weights (w_i) are the weight of evidence in favor of model i being the actual best model given that one of the N models must be the best model for that set of N models. Additionally, we computed a likelihood ratio test (Vuong, 1989; Clauset *et al.*, 2009) of the power law model against the other distributions. We calculated bootstrapped 95% confidence intervals (Crawley, 2012) for the parameters of the best model, using the bias-corrected and accelerated (BCa) bootstrap (Efron & Tibshirani, 1994) with 10000 replications.

Largest patch dynamics

The largest patch is the one that connects the highest number of sites in the area. This has been used extensively to indicate fragmentation (Gardner & Urban, 2007; Ochoa-Quintero *et al.*, 2015). The relation of the size of the largest patch S_{max} to critical transitions has been extensively studied in relation to percolation phenomena (Stauffer & Aharony, 1994; Bazant, 2000; Botet & Ploszajczak, 2004), but is seldom used in ecological studies (for an exception see Gastner *et al.* (2009)). When the system is in a connected state ($p > p_c$) the landscape is almost insensitive to the loss of a small fraction of forest, but close to the critical point a minor loss can have important effects (Solé & Bascompte, 2006; Oborny *et al.*, 2007), because at this point the largest patch will have a filamentary structure, i.e. extended forest areas will be connected by thin threads. Small losses can thus produce large fluctuations.

One way to evaluate the fragmentation of the forest is to calculate the proportion of the largest patch against the total area (Keitt *et al.*, 1997). The total area of the regions we are considering (Appendix S4, figures S1-S6) may not be the same than the total area that the forest could potentially occupy, and thus a more

bioRxiv preprint doi: https://doi.org/10.1101/091751; this version posted January 9, 2018. The copyright holder for this preprint (which was not certified by peer review) is the author/funder. All rights reserved. No reuse allowed without permission.

accurate way to evaluate the weight of S_{max} is to use the total forest area, which can be easily calculated by summing all the forest pixels. We calculate the proportion of the largest patch for each year, dividing S_{max} by the total forest area of the same year: $RS_{max} = S_{max}/\sum_i S_i$. This has the effect of reducing the S_{max} fluctuations produced due to environmental or climatic changes influences in total forest area. When the proportion RS_{max} is large (more than 60%) the largest patch contains most of the forest so there are fewer small forest patches and the system is probably in a connected phase. Conversely, when it is low (less than 20%), the system is probably in a fragmented phase (Saravia & Momo, 2017). To define if a region will be in a connected or unconnected state we used the RS_{max} of the highest (i.e., most conservative) threshold of 40%, that represent the most dense area of forest within our chosen range. We assume that there are two alternative states for the critical transition–the forest could be fragmented or unfragmented. If RS_{max} is a good indicator of the fragmentation state of the forest its distribution of frequencies should be bimodal (Bestelmeyer *et al.*, 2011), so we apply the Hartigan's dip test that measures departures from unimodality (Hartigan & Hartigan, 1985).

The RS_{max} is a useful qualitative index that does not tell us if the system is near or far from the critical transition; this can be evaluated using the temporal fluctuations. We calculate the fluctuations around the mean with the absolute values $\Delta S_{max} = S_{max}(t) - \langle S_{max} \rangle$, using the proportions of RS_{max}. To characterize fluctuations we fitted three empirical distributions: power-law, log-normal, and exponential, using the same methods described previously. We expect that large fluctuation near a critical point have heavy tails (log-normal or power-law) and that fluctuations far from a critical point have exponential tails, corresponding to Gaussian processes (Rooij *et al.*, 2013). As the data set spans 16 years, it is probable that will do not have enough power to reliably detect which distribution is better (Clauset *et al.*, 2009). To improve this we used the same likelihood ratio test we used previously (Vuong, 1989; Clauset *et al.*, 2009); if the p-value obtained to compare the best distribution against the others we concluded that there is not enough data to decide which is the best model. We generated animated maps showing the fluctuations of the two largest patches at 30% threshold, to aid in the interpretations of the results.

A robust way to detect if the system is near a critical transition is to analyze the increase in variance of the density (Benedetti-Cecchi *et al.*, 2015). It has been demonstrated that the variance increase in density appears when the system is very close to the transition (Corrado *et al.*, 2014), and thus practically it does not constitute an early warning indicator. An alternative is to analyze the variance of the fluctuations of the largest patch ΔS_{max}: the maximum is attained at the critical point but a significant increase occurs well before the system reaches the critical point (Corrado *et al.*, 2014; Saravia & Momo, 2017). In addition, before the critical fragmentation, the skewness of the distribution of ΔS_{max} should be negative, implying

bioRxiv preprint doi: https://doi.org/10.1101/091751; this version posted January 9, 2018. The copyright holder for this preprint (which was not certified by peer review) is the author/funder. All rights reserved. No reuse allowed without permission.

that fluctuations below the average are more frequent. We characterized the increase in the variance using quantile regression: if variance is increasing the slopes of upper or/and lower quartiles should be positive or negative.

All statistical analyses were performed using the GNU R version 3.3.0 (R Core Team, 2015), to fit the distributions of patch sizes we used the Python package powerlaw (Alstott *et al.*, 2014). For the quantile regressions we used the R package quantreg (Koenker, 2016). Image processing was done in MATLAB r2015b (The Mathworks Inc.). The complete source code for image processing and statistical analysis, and the patch size data files are available at figshare http://dx.doi.org/10.6084/m9.figshare.4263905.

Results

The figure 1 shows an example of the distribution of the biggest 200 patches for years 2000 and 2014. This distribution is highly variable; the biggest patch usually maintains its spatial location, but sometimes it breaks and then big fluctuations in its size are observed, as we will analyze below. Smaller patches can merge or break more easily so they enter or leave the list of 200, and this is why there is a color change across years.

The power law distribution was selected as the best model in 99% of the cases (Figure S7). In a small number of cases (1%) the power law with exponential cutoff was selected, but the value of the parameter α was similar by ± 0.03 to the pure power law (Table S1, and model fit data table). Additionally the patch size where the exponential tail begins is very large, and thus we used the power law parameters for these cases (region EUAS3,SAST2). In finite-size systems the favored model should be the power law with exponential cut-off, because the power-law tails are truncated to the size of the system (Stauffer & Aharony, 1994). This implies that differences between the two kinds of power law models should be small. We observe this effect: when the pure power-law model is selected as the best model the likelihood ratio test shows that in 64% of the cases the differences with power law with exponential cutoff are not significant (p-value$>$0.05); in these cases the differences between the fitted α for both models are less than 0.001. Instead the likelihood ratio test clearly differentiates the power law model from the exponential model (100% cases p-value$<$0.05), and the log-normal model (90% cases p-value$<$0.05).

The global mean of the power-law exponent α is 1.967 and the bootstrapped 95% confidence interval is 1.964 - 1.970. The global values for each threshold are different, because their confidence intervals do not overlap, and their range goes from 1.90 to 2.01 (Table S1). Analyzing the biggest regions (Figure 1, Table S2) the northern hemisphere regions (EUAS1 & NA1) have similar values of α (1.97, 1.98), pantropical areas

bioRxiv preprint doi: https://doi.org/10.1101/091751; this version posted January 9, 2018. The copyright holder for this preprint (which was not certified by peer review) is the author/funder. All rights reserved. No reuse allowed without permission.

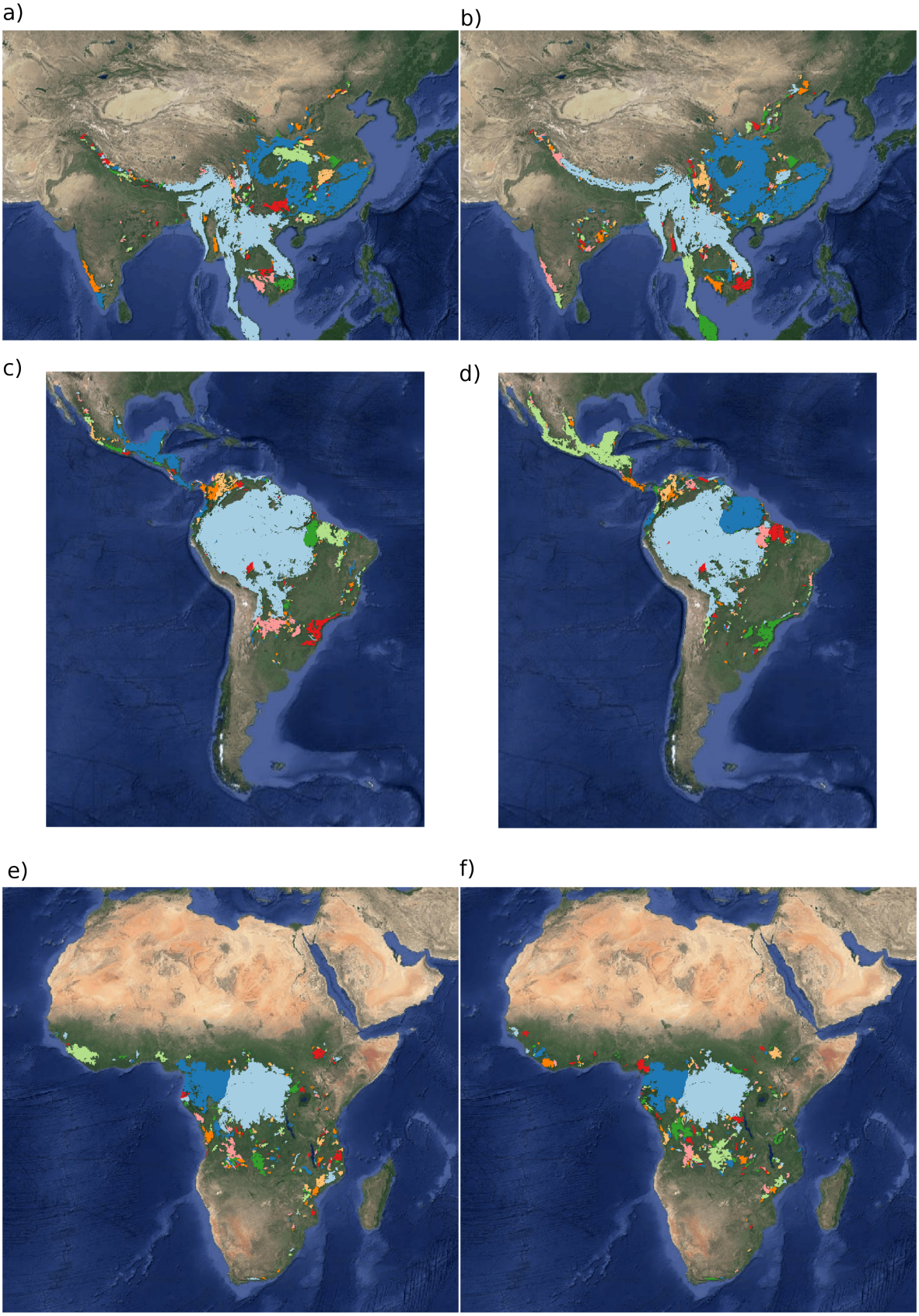

Figure 1: Forest patch distributions for continental regions for the years 2000 and 2014. The images are the 200 biggest patches, shown at a coarse pixel scale of 2.5 km. The regions are: a) & b) southeast Asia; c) & d) South America subtropical and tropical and e) & f) Africa mainland, for the years 2000 and 2014 respectively. The color palette was chosen to discriminate different patches and does not represent patch size.

bioRxiv preprint doi: https://doi.org/10.1101/091751; this version posted January 9, 2018. The copyright holder for this preprint (which was not certified by peer review) is the author/funder. All rights reserved. No reuse allowed without permission.

have different α with greatest values for South America (SAST1, 2.01) and in descending order Africa (AF1, 1.946) and Southeast Asia (SEAS1, 1.895). With greater α the fluctuations of patch sizes are lower and vice versa (Newman, 2005).

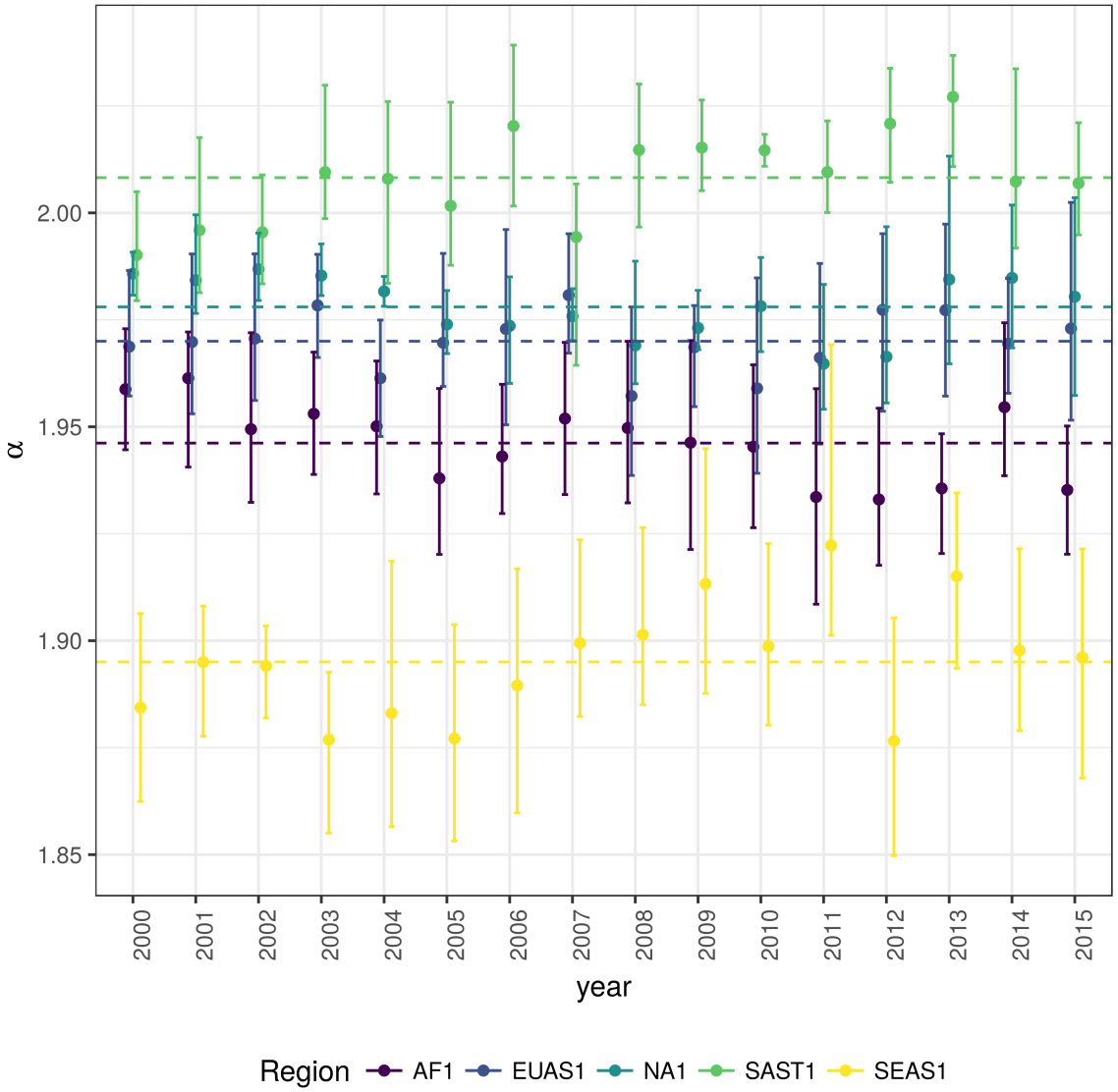

Figure 2: Power law exponents (α) of forest patch distributions for regions with total forest area $> 10^7$ km^2. Dashed horizontal lines are the means by region, with 95% confidence interval error bars estimated by bootstrap resampling. The regions are AF1: Africa mainland, EUAS1: Eurasia mainland, NA1: North America mainland, SAST1: South America subtropical and tropical, SEAS1: Southeast Asia mainland.

We calculated the total areas of forest and the largest patch S_{max} by year for different thresholds, and as expected these two values increase for smaller thresholds (Table S3). We expect fewer variations in the largest patch relative to total forest area RS_{max} (Figure S9); in ten cases it stayed near or higher than 60% (EUAS2, NA5, OC2, OC3, OC4, OC5, OC6, OC8, SAST1, SAT1) over the 25-35 range or more. In four

bioRxiv preprint doi: https://doi.org/10.1101/091751; this version posted January 9, 2018. The copyright holder for this preprint (which was not certified by peer review) is the author/funder. All rights reserved. No reuse allowed without permission.

cases it stayed around 40% or less, at least over the 25-30% range (AF1, EUAS3, OC1, SAST2), and in six cases there is a crossover from more than 60% to around 40% or less (AF2, EUAS1, NA1, OC7, SEAS1, SEAS2). This confirms the criteria of using the most conservative threshold value of 40% to interpret RS_{max} with regard to the fragmentation state of the forest. The frequency of RS_{max} showed bimodality (Figure 3) and the dip test rejected unimodality (D = 0.0416, p-value = 0.0003), which also implies that RS_{max} is a good index to study the fragmentation state of the forest.

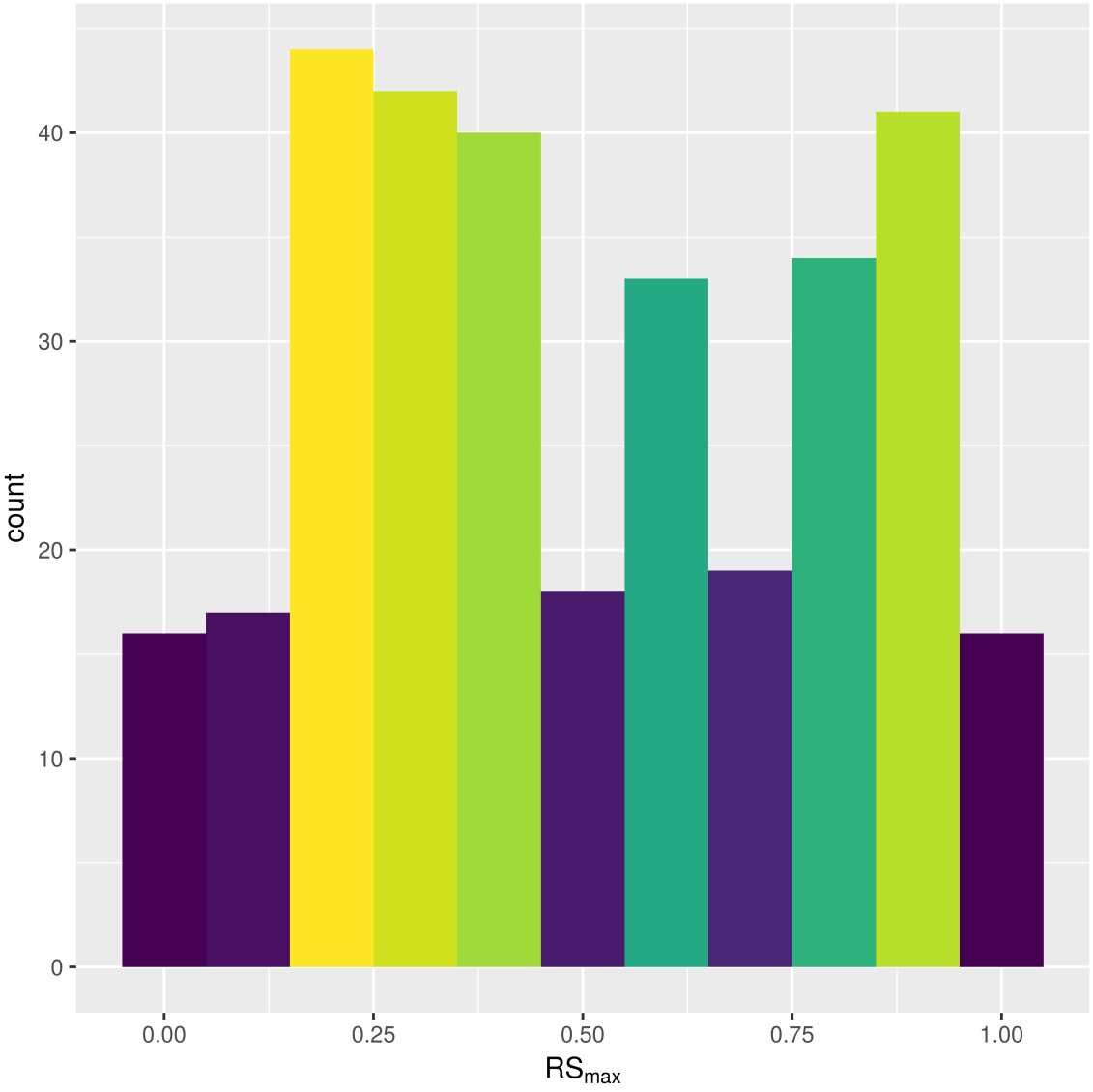

Figure 3: Frequency distribution of Largest patch proportion relative to total forest area RS_{max} calculated using a threshold of 40% of forest in each pixel to determine patches. Bimodality is observed and confirmed by the dip test (D = 0.0416, p-value = 0.0003).This indicates the existence of two states needed for a critical transition.

The RS_{max} for regions with more than 10^7 km^2 of forest is shown in figure 4. South America tropical and

bioRxiv preprint doi: https://doi.org/10.1101/091751; this version posted January 9, 2018. The copyright holder for this preprint (which was not certified by peer review) is the author/funder. All rights reserved. No reuse allowed without permission.

subtropical (SAST1) is the only region with an average close to 60%, the other regions are below 30%. Eurasia mainland (EUAS1) has the lowest value near 20%. For regions with less total forest area (Figure S10, Table S3), Great Britain (EUAS3) has the lowest proportion less than 5%, Java (OC7) and Cuba (SAST2) are under 25%, while other regions such as New Guinea (OC2), Malaysia/Kalimantan (OC3), Sumatra (OC4), Sulawesi (OC5) and South New Zealand (OC6) have a very high proportion (75% or more). Philippines (SEAS2) seems to be a very interesting case because it seems to be under 30% until the year 2007, fluctuates around 30% in years 2008-2010, then jumps near 60% in 2011-2013 and then falls again to 30%, this seems an example of a transition from a fragmented state to a unfragmented one (figure S10).

We analyzed the distributions of fluctuations of the largest patch relative to total forest area ΔRS_{max} and the fluctuations of the largest patch ΔS_{max}. Although the Akaike criteria identified different distributions as the best, in most cases the Likelihood ratio test was not significant and we are not able, from these data, to determine with confidence which is the best distribution. In only one case was the distribution selected by the Akaike criteria confirmed as the correct model for relative and absolute fluctuations (Table S4).

The animations of the two largest patches (see supplementary data, largest patch gif animations) qualitatively shows the nature of fluctuations and if the state of the forest is connected or not. If the largest patch is always the same patch over time, the forest is probably not fragmented; this happens for regions with RS_{max} of more than 40% such as AF2 (Madagascar), EUAS2 (Japan), NA5 (Newfoundland) and OC3 (Malaysia). In regions with RS_{max} between 40% and 30% the identity of the largest patch could change or stay the same in time. For OC7 (Java) the largest patch changes and for AF1 (Africa mainland) it stays the same. Only for EUAS1 (Eurasia mainland) did we observe that the two largest patches are always the same, implying that this region is probably composed of two independent domains and should be sub-divided in future studies. The regions with RS_{max} less than 25% included SAST2 (Cuba) and EUAS3 (Great Britain); in these cases the always-changing largest patch reflects their fragmented state. In the case of SEAS2 (Philippines) a transition is observed, with the identity of the largest patch first variable, and then constant after 2010.

The results of quantile regressions are almost identical for ΔRS_{max} and ΔS_{max} (table S5). Among the biggest regions, Africa (AF1) has a similar pattern across thresholds but only the 30% threshold is significant; the upper and lower quantiles have significant negative slopes, but the lower quantile slope is lower, implying that negative fluctuations and variance are increasing (Figure 5). Eurasia mainland (EUAS1) has significant slopes at 20%, 30% and 40% thresholds but the patterns are different at 20% variance is decreasing, at 30% and 40% only is increasing. Thus the variation of the most dense portion of the largest patch is increasing within a limited range. North America mainland (NA1) exhibits the same pattern at 20%, 25% and 30% thresholds: a significant lower quantile with positive slope, implying decreasing variance. South

bioRxiv preprint doi: https://doi.org/10.1101/091751; this version posted January 9, 2018. The copyright holder for this preprint (which was not certified by peer review) is the author/funder. All rights reserved. No reuse allowed without permission.

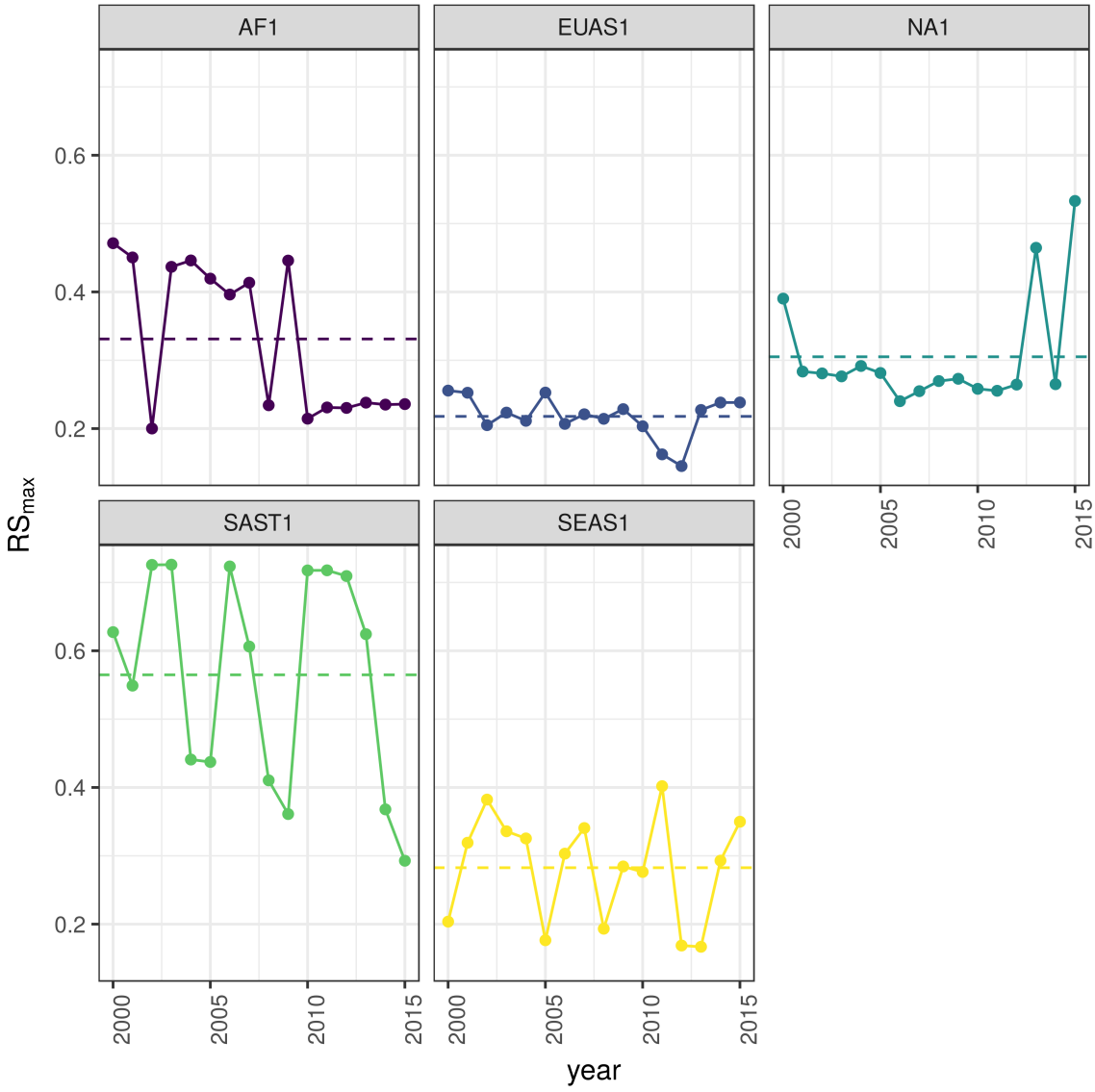

Figure 4: Largest patch proportion relative to total forest area RS_{max}, for regions with total forest area $> 10^7$ km^2. We show here the RS_{max} calculated using a threshold of 40% of forest in each pixel to determine patches. Dashed lines are averages across time. The regions are AF1: Africa mainland, EUAS1: Eurasia mainland, NA1: North America mainland, SAST1: South America tropical and subtropical, SEAS1: Southeast Asia mainland.

bioRxiv preprint doi: https://doi.org/10.1101/091751; this version posted January 9, 2018. The copyright holder for this preprint (which was not certified by peer review) is the author/funder. All rights reserved. No reuse allowed without permission.

America tropical and subtropical (SAST1) have significant lower quantile with negative slope at 25% and 30% thresholds indicating an increase in variance. SEAS1 has an upper quantile with positive slope significant for 25% threshold, also indicating an increasing variance. The other regions, with forest area smaller than 10^7km^2 are shown in figure S11 and table S5. Philippines (SEAS2) is an interesting case: the slopes of lower quantiles are positive for thresholds 20% and 25%, and the upper quantile slopes are positive for thresholds 30% and 40$; thus variance is decreasing at 20%-25% and increasing at 30%-40%.

The conditions that indicate that a region is near a critical fragmentation threshold are that patch size distributions follow a power law; variance of ΔRS_{max} is increasing in time; and skewness is negative. All these conditions must happen at the same time at least for one threshold. When the threshold is higher more dense regions of the forest are at risk. This happens for Africa mainland (AF1), Eurasia mainland(EUAS1), Japan (EUAS2), Australia mainland (OC1), Malaysia/Kalimantan (OC3), Sumatra (OC4), South America tropical & subtropical (SAST1), Cuba (SAST2), Southeast Asia, Mainland (SEAS1).

bioRxiv preprint doi: https://doi.org/10.1101/091751; this version posted January 9, 2018. The copyright holder for this preprint (which was not certified by peer review) is the author/funder. All rights reserved. No reuse allowed without permission.

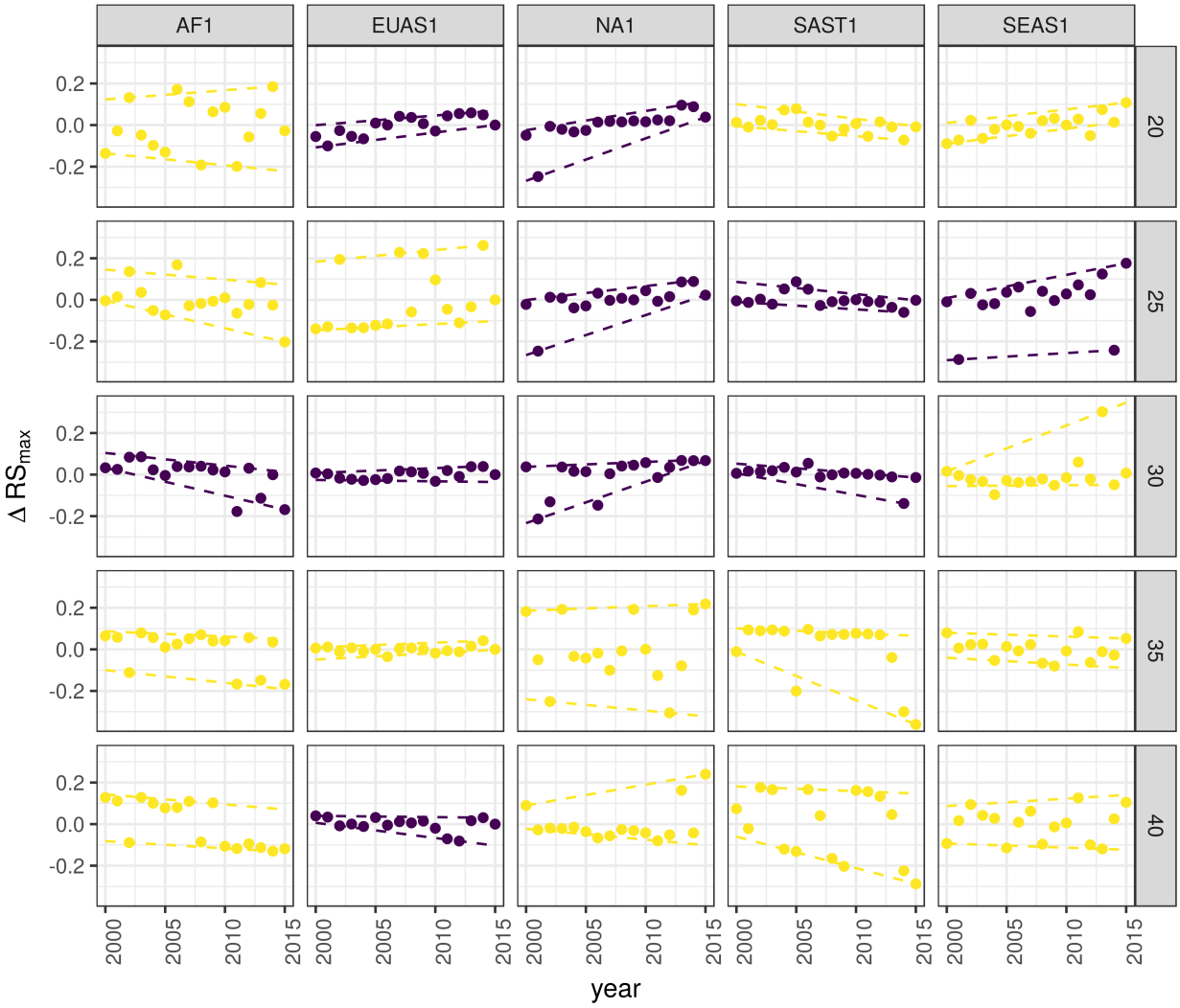

Figure 5: Largest patch fluctuations for regions with total forest area $> 10^7 \text{km}^2$ across years. The patch sizes are relative to the total forest area of the same year. Dashed lines are 90% and 10% quantile regressions, to show if fluctuations were increasing; purple (dark) panels have significant slopes. The regions are AF1: Africa mainland, EUAS1: Eurasia mainland, NA1: North America mainland, SAST1: South America tropical and subtropical, SEAS1: Southeast Asia mainland.

bioRxiv preprint doi: https://doi.org/10.1101/091751; this version posted January 9, 2018. The copyright holder for this preprint (which was not certified by peer review) is the author/funder. All rights reserved. No reuse allowed without permission.

Table 1: Regions and indicators of closeness to a critical fragmentation point. Where: RS_{max} is the largest patch divided by the total forest area; Threshold is the value used to calculate patches from the MODIS VCF pixels; ΔRS_{max} are the fluctuations of RS_{max} around the mean and and the increase or decrease in the variance was estimated using quantile regressions; skewness was calculated for RS_{max}. NS means the results were non-significant. The conditions that determine the closeness to a fragmentation point are: increasing variance of ΔRS_{max} and negative skewness. RS_{max} indicates if the forest is unfragmented (>0.6) or fragmented (<0.3).

Region	Description	RS_{max}	Threshold	Variance of ΔRS_{max}	Skewness
AF1	Africa mainland	0.33	30	Increase	-1.4653
AF2	Madagascar	0.48	20	Increase	0.7226
EUAS1	Eurasia, mainland	0.22	20	Decrease	-0.4814
EUAS1			30	Increase	0.3113
EUAS1			40	Increase	-1.2790
EUAS2	Japan	0.94	35	Increase	-0.3913
EUAS2			40	Increase	-0.5030
EUAS3	Great Britain	0.03	40	NS	
NA1	North America, mainland	0.31	20	Decrease	-2.2895
NA1			25	Decrease	-2.4465
NA1			30	Decrease	-1.6340
NA5	Newfoundland	0.54	40	NS	
OC1	Australia, Mainland	0.36	30	Increase	0.0920
OC1			35	Increase	-0.8033
OC2	New Guinea	0.96	25	Decrease	-0.1003
OC2			30	Decrease	0.1214
OC2			35	Decrease	-0.0124
OC3	Malaysia/Kalimantan	0.92	35	Increase	-1.0147
OC3			40	Increase	-1.5649
OC4	Sumatra	0.84	20	Increase	-1.3846
OC4			25	Increase	-0.5887
OC4			30	Increase	-1.4226
OC5	Sulawesi	0.82	40	NS	
OC6	New Zealand South Island	0.75	40	Increase	0.3553
OC7	Java	0.16	40	NS	
OC8	New Zealand North Island	0.64	40	NS	
SAST1	South America, Tropical and Subtropical forest	0.56	25	Increase	1.0519
SAST1			30	Increase	-2.7216
SAST2	Cuba	0.15	20	Increase	0.5049
SAST2			25	Increase	1.7263
SAST2			30	Increase	0.1665
SAST2			40	Increase	-0.5401
SAT1	South America, Temperate forest	0.54	25	Decrease	0.1483
SAT1			30	Decrease	-1.6059
SAT1			35	Decrease	-1.3809
SEAS1	Southeast Asia, Mainland	0.28	25	Increase	-1.3328
SEAS2	Philippines	0.33	20	Decrease	-1.6373
SEAS2			25	Decrease	-0.6648
SEAS2			30	Increase	0.1517

bioRxiv preprint doi: https://doi.org/10.1101/091751; this version posted January 9, 2018. The copyright holder for this preprint (which was not certified by peer review) is the author/funder. All rights reserved. No reuse allowed without permission.

Region	Description	RS_{max}	Threshold	Variance of ΔRS_{max}	Skewness
SEAS2			40	Increase	1.5996

Discussion

We found that the forest patch distribution of all regions of the world, spanning tropical rainforests, boreal and temperate forests, followed power laws spanning seven orders of magnitude. Power laws have previously been found for several kinds of vegetation, but never at global scales as in this study. Moreover the range of the estimated power law exponents is relatively narrow (1.90 - 2.01), even though we tested a variety of different thresholds levels. This suggest the existence of one unifying mechanism, or perhaps different mechanisms that act in the same way in different regions, affecting forest spatial structure and dynamics.

Several mechanisms have been proposed for the emergence of power laws in forests. The first is related self organized criticality (SOC), when the system is driven by its internal dynamics to a critical state; this has been suggested mainly for fire-driven forests (Zinck & Grimm, 2009; Hantson *et al.*, 2015). Real ecosystems do not seem to meet the requirements of SOC dynamics (Pueyo *et al.*, 2010; McKenzie & Kennedy, 2012), however, because they have both endogenous and exogenous controls, are non-homogeneous, and do not have a separation of time scales [Solé *et al.* (2002);Sole2006]. A second possible mechanism, suggested by Pueyo et al. (2010), is isotropic percolation: when a system is near the critical point, the power law structures arise. This is equivalent to the random forest model that we explained previously, and requires the tuning of an external environmental condition to carry the system to this point. We did not expect forest growth to be a random process at local scales, but it is possible that combinations of factors cancel out to produce seemingly random forest dynamics at large scales. In this case we should have observed power laws in a limited set of situations that coincide with a critical point, but instead we observed pervasive power law distributions. Thus isotopic percolation does not seem likely to be the mechanism that produces the observed distributions. A third possible mechanism is facilitation (Manor & Shnerb, 2008; Irvine *et al.*, 2016): a patch surrounded by forest will have a smaller probability of being deforested or degraded than an isolated patch. The model of Scanlon et al. (2007) showed an $\alpha = 1.34$ which is different from our results (1.90 - 2.01 range). Another model but with three states (tree/non-tree/degraded), including local facilitation and grazing, was also used to obtain power laws patch distributions without external tuning, and exhibited deviations from power laws at high grazing pressures (Kéfi *et al.*, 2007). The values of the power law exponent α obtained for this model are dependent on the intensity of facilitation: when facilitation is more intense the exponent is higher, but the maximal values they obtained are still lower than the ones we observed. The interesting point is that

bioRxiv preprint doi: https://doi.org/10.1101/091751; this version posted January 9, 2018. The copyright holder for this preprint (which was not certified by peer review) is the author/funder. All rights reserved. No reuse allowed without permission.

the value of the exponent is dependent on the parameters, and thus the observed α might be obtained with some parameter combination.

The existence of possible critical transitions in forests, mainly in neotropical forest to savanna, is a matter of intense investigation, with the transitions generally thought to be first order or discontinuous transitions. Here, however, we found power laws in forest patch distributions, implying (i.e., a necessary but not a sufficient condition) a second order or continuous transition. A power law patch distribution can be indicative of a critical transition if it is present in a narrow range of conditions; conversely, if it is not found, the existence of a critical transition cannot be discarded. New research (Villa Martín *et al.*, 2014, 2015) has suggested that first order transitions do not even exist when the system is (i) spatially heterogeneous and (ii) exhibits internal and external stochastic fluctuations, as in forests. Thus the application of indices based on second order transitions seems to be justified.

It has been suggested that a combination of spatial and temporal indicators could more reliably detect critical transitions (Kéfi *et al.*, 2014). In this study, we combined five criteria to evaluate the closeness of the system to a fragmentation threshold. Two of them were spatial: the forest patch size distribution, and the proportion of the largest patch relative to total forest area RS_{max}. The other three were the distribution of temporal fluctuations in the largest patch size, the trend in the variance, and the skewness of the fluctuations. One of them: the distribution of temporal fluctuations ΔRS_{max} can not be applied with our temporal resolution due to the difficulties of fitting and comparing heavy tailed distributions. The combination of the remaining four gives us an increased degree of confidence about the system being close to a critical transition.

Monitoring the biggest patches using RS_{max} is also important regardless of the existence or not of critical transitions. RS_{max} is relative to total forest area thus it could be used to compare regions with a different extension of forests and as the total area of forest also changes with different environmental conditions, e.g. this could be used to compare forest from different latitudes. Moreover, the areas covered by S_{max} across regions contain most of the intact forest landscapes defined by Potapov *et al.* (2008a), and thus RS_{max} is a relatively simple way to evaluate the risk in these areas.

This analysis is at scale of continents so it is in fact a macrosystems analysis (Heffernan *et al.*, 2014), in which it is important to link local processes with resulting larger-scale (here, continental) patterns. Here, we identified macro-scale dynamical patterns that deserve attention. To link these patterns across scales requires a substantial amount of investigation, probably performing the same analysis for smaller regions that identify more clearly which kind of forest and processes are locally involved. We know that the same procedure could be applied to local scales because the patch distributions are power laws; power law distributions are self-

bioRxiv preprint doi: https://doi.org/10.1101/091751; this version posted January 9, 2018. The copyright holder for this preprint (which was not certified by peer review) is the author/funder. All rights reserved. No reuse allowed without permission.

similar, or invariant to scale changes. Thus unless power law distribution are broken we could apply the same methodology to more local scales.

South America tropical and subtropical (SAST1), Southeast Asia mainland (SEAS1) and Africa mainland (AF1) met all criteria at least for one threshold; these regions generally experience the biggest rates of deforestation with a significant increase in loss of forest (Hansen *et al.*, 2013). From our point of view the most critical region is Southeast Asia, because the proportion of the largest patch relative to total forest area RS_{max} was 28%. This suggests that Southeast Asia's forests are the most fragmented, and thus its flora and fauna the most endangered. Due to the criteria we adopted to define regions, we could not detect the effect of conservation policies applied at a country level, e.g. the Natural Forest Conservation Program in China, which has produced an 1.6% increase in forest cover and net primary productivity over the last 20 years (Viña *et al.*, 2016). Indonesia and Malaysia (OC3) both are countries with hight deforestation rates (Hansen *et al.*, 2013); Sumatra (OC4) is the biggest island of Indonesia and where most deforestation occurs. Both regions show a high RS_{max} greater than 60%, and thus the forest is in an unfragmented state, but they met all other criteria, meaning that they are approaching a transition if the actual deforestation rates continue. At present our indices are qualitative but we expect to develop them in a more quantitative way to predict how many years would be needed to complete a critical transition if actual forest loss rates are maintained.

The Eurasian mainland region (EUAS1) is an extensive area with mainly temperate and boreal forest, and a combination of forest loss due to fire (Potapov *et al.*, 2008b) and forestry. The biggest country is Russia that experienced the biggest rate of forest loss of all countries, but here in the zone of coniferous forest the the largest gain is observed due to agricultural abandonment (Prishchepov *et al.*, 2013). The loss is maximum at the most dense areas of forest (Hansen *et al.*, 2013, Table S3), this coincides with our analysis that detect an increasing risk at denser forest. This region also has a relatively low RS_{max} that means is probably near a fragmented state. A region that is similar in forest composition to EAUS1 is North America (NA1); the two main countries involved, United States and Canada, have forest dynamics mainly influenced by fire and forestry, with both regions are extensively managed for industrial wood production. North America has a higher RS_{max} than Eurasia and a positive skewness that excludes it from being near a critical transition. A possible explanation of this is that in Russia after the collapse of the Soviet Union harvest was lower due to agricultural abandonment but illegal overharvesting of high valued stands has increased in recent decades (Gauthier *et al.*, 2015).

The analysis of RS_{max} reveals that the island of Philippines (SEAS2) seems to be an example of a critical transition from an unconnected to a connected state, i.e. from a state with high fluctuations and low RS_{max}

bioRxiv preprint doi: https://doi.org/10.1101/091751; this version posted January 9, 2018. The copyright holder for this preprint (which was not certified by peer review) is the author/funder. All rights reserved. No reuse allowed without permission.

to a state with low fluctuations and high RS_{max}. If we observe this pattern backwards in time, the decrease in variance increases, and negative skewness is constant, and thus the region exhibits the criteria of a critical transition (Table 1, Figure S11). The actual pattern of transition to an unfragmented state could be the result of an active intervention of the government promoting conservation and rehabilitation of protected areas, ban of logging old-growth forest, reforestation of barren areas, community-based forestry activities, and sustainable forest management in the country's production forest (Lasco *et al.*, 2008). This confirms that the early warning indicators proposed here work in the correct direction. An important caveat is that the MODIS dataset does not detect if native forest is replaced by agroindustrial tree plantations like oil palms, that are among the main drivers of deforestation in this area (Malhi *et al.*, 2014). To improve the estimation of forest patches, data sets as the MODIS cropland probability and others about land use, protected areas, forest type, should be incorporated (Hansen *et al.*, 2014; Sexton *et al.*, 2015).

Deforestation and fragmentation are closely related. At low levels of habitat reduction species population will decline proportionally; this can happen even when the habitat fragments retain connectivity. As habitat reduction continues, the critical threshold is approached and connectivity will have large fluctuations (Brook *et al.*, 2013). This could trigger several negative synergistic effects: population fluctuations and the possibility of extinctions will rise, increasing patch isolation and decreasing connectivity (Brook *et al.*, 2013). This positive feedback mechanism will be enhanced when the fragmentation threshold is reached, resulting in the loss of most habitat specialist species at a landscape scale (Pardini *et al.*, 2010). Some authors have argued that since species have heterogeneous responses to habitat loss and fragmentation, and biotic dispersal is limited, the importance of thresholds is restricted to local scales or even that its existence is questionable (Brook *et al.*, 2013). Fragmentation is by definition a local process that at some point produces emergent phenomena over the entire landscape, even if the area considered is infinite (Oborny *et al.*, 2005). In addition, after a region's fragmentation threshold connectivity decreases, there is still a large and internally well connected patch that can maintain sensitive species (Martensen *et al.*, 2012). What is the time needed for these large patches to become fragmented, and pose a real danger of extinction to a myriad of sensitive species? If a forest is already in a fragmented state, a second critical transition from forest to non-forest could happen: the desertification transition (Corrado *et al.*, 2014). Considering the actual trends of habitat loss, and studying the dynamics of non-forest patches—instead of the forest patches as we did here—the risk of this kind of transition could be estimated. The simple models proposed previously could also be used to estimate if these thresholds are likely to be continuous and reversible or discontinuous and often irreversible (Weissmann & Shnerb, 2016), and the degree of protection (e.g. using the set-asides strategy Banks-Leite *et al.* (2014)) that would be necessary to stop this trend.

bioRxiv preprint doi: https://doi.org/10.1101/091751; this version posted January 9, 2018. The copyright holder for this preprint (which was not certified by peer review) is the author/funder. All rights reserved. No reuse allowed without permission.

The effectiveness of landscape management is related to the degree of fragmentation, and the criteria to direct reforestation efforts could be focused on regions near a transition (Oborny *et al.*, 2007). Regions that are in an unconnected state require large efforts to recover a connected state, but regions that are near a transition could be easily pushed to a connected state; feedbacks due to facilitation mechanisms might help to maintain this state. Crossing the fragmentation critical point in forests could have negative effects on biodiversity and ecosystem services (Haddad *et al.*, 2015), but it could also produce feedback loops at different levels of the biological hierarchy. This means that a critical transition produced at a continental scale could have effects at the level of communities, food webs, populations, phenotypes and genotypes (Barnosky *et al.*, 2012). All these effects interact with climate change, thus there is a potential production of cascading effects that could lead to an abrupt climate change with potentially large ecological and economic impact (Alley *et al.*, 2003).

Therefore, even if critical thresholds are reached only in some forest regions at a continental scale, a cascading effect with global consequences could still be produced (Reyer *et al.*, 2015). The risk of such event will be higher if the dynamics of separate continental regions are coupled (Lenton & Williams, 2013). At least three of the regions defined here are considered tipping elements of the earth climate system that could be triggered during this century (Lenton *et al.*, 2008). These were defined as policy relevant tipping elements so that political decisions could determine whether the critical value is reached or not. Thus using the criteria proposed here could be used as a more sensitive system to evaluate the closeness of a tipping point at a continental scale, but the same criteria could also be uses to evaluate local problems at smaller areas. Further improvements will produce quantitative predictions about the temporal horizon where these critical transitions could produce significant changes in the studied systems.

Supporting information

Appendix

Table S1: Mean power-law exponent and Bootstrapped 95% confidence intervals by threshold.

Table S2: Mean power-law exponent and Bootstrapped 95% confidence intervals across thresholds by region and year.

Table S3: Mean total patch area; largest patch S_{max} in km^2; largest patch propotional to total patch area RS_{max} and 95% bootstrapped confidence interval of RS_{max}, by region and thresholds, averaged across years

Table S4: Model selection for distributions of fluctuation of largest patch ΔS_{max} and largest patch relative to total forest area ΔRS_{max}.

bioRxiv preprint doi: https://doi.org/10.1101/091751; this version posted January 9, 2018. The copyright holder for this preprint (which was not certified by peer review) is the author/funder. All rights reserved. No reuse allowed without permission.

Table S5: Quantil regressions of the fluctuations of the largest patch vs year, for 10% and 90% quantils at different pixel thresholds.

Table S6: Unbiased estimation of Skewness of fluctuations of the largest patch ΔS_{max} and fluctuations relative to total forest area ΔRS_{max}.

Figure S1: Regions for Africa: Mainland (AF1), Madagascar (AF2).

Figure S2: Regions for Eurasia: Mainland (EUAS1), Japan (EUAS2), Great Britain (EUAS3).

Figure S3: Regions for North America: Mainland (NA1), Newfoundland (NA5).

Figure S4: Regions for Australia and islands: Australia mainland (OC1), New Guinea (OC2), Malaysia/Kalimantan (OC3), Sumatra (OC4), Sulawesi (OC5), New Zealand south island (OC6), Java (OC7), New Zealand north island (OC8).

Figure S5: Regions for South America: Tropical and subtropical forest up to Mexico (SAST1), Cuba (SAST2), South America Temperate forest (SAT1).

Figure S6: Regions for Southeast Asia: Mainland (SEAS1), Philippines (SEAS2).

Figure S7: Proportion of best models selected for patch size distributions using the Akaike criterion.

Figure S8: Power law exponents for forest patch distributions by year for all regions.

Figure S9: Average largest patch relative to total forest area RS_{max} by threshold, for all regions.

Figure S10: Largest patch relative to total forest area RS_{max} by year at 40% threshold, for regions with total forest area less than 10^7 km^2.

Figure S11: Fluctuations of largest patch relative to total forest area RS_{max} for regions with total forest area less than 10^7 km^2 by year and threshold.

Data Accessibility

The MODIS VCF product is freely available from NASA at https://search.earthdata.nasa.gov/. Csv text file with model fits for patch size distribution, and model selection for all the regions; Gif Animations of a forest model percolation; Gif animations of largest patches; patch size files for all years and regions used here; and all the R, Python and Matlab scripts are available at figshare http://dx.doi.org/10.6084/m9.figshare.4263905.

bioRxiv preprint doi: https://doi.org/10.1101/091751; this version posted January 9, 2018. The copyright holder for this preprint (which was not certified by peer review) is the author/funder. All rights reserved. No reuse allowed without permission.

Acknowledgments

LAS and SRD are grateful to the National University of General Sarmiento for financial support. We want to thank to Jordi Bascompte, Nara Guisoni, Fernando Momo, and two anonymous reviewers for their comments and discussions that greatly improved the manuscript. This work was partially supported by a grant from CONICET (PIO 144-20140100035-CO).

References

Alley RB, Marotzke J, Nordhaus WD et al. (2003) Abrupt Climate Change. *Science*, **299**, 2005–2010.

Allington GRH, Valone TJ (2010) Reversal of desertification: The role of physical and chemical soil properties. *Journal of Arid Environments*, **74**, 973–977.

Alstott J, Bullmore E, Plenz D (2014) powerlaw: A Python Package for Analysis of Heavy-Tailed Distributions. *PLOS ONE*, **9**, e85777.

Angelsen A (2010) Policies for reduced deforestation and their impact on agricultural production. *Proceedings of the National Academy of Sciences*, **107**, 19639–19644.

Banks-Leite C, Pardini R, Tambosi LR et al. (2014) Using ecological thresholds to evaluate the costs and benefits of set-asides in a biodiversity hotspot. *Science*, **345**, 1041–1045.

Barnosky AD, Hadly EA, Bascompte J et al. (2012) Approaching a state shift in Earth's biosphere. *Nature*, **486**, 52–58.

Bascompte J, Solé RV (1996) Habitat fragmentation and extinction threholds in spatially explicit models. *Journal of Animal Ecology*, **65**, 465–473.

Bazant MZ (2000) Largest cluster in subcritical percolation. *Physical Review E*, **62**, 1660–1669.

Belward AS (1996) The IGBP-DIS Global 1 Km Land Cover Data Set "DISCover": Proposal and Implementation Plans : Report of the Land Recover Working Group of IGBP-DIS. IGBP-DIS Office, pp.

Benedetti-Cecchi L, Tamburello L, Maggi E, Bulleri F (2015) Experimental Perturbations Modify the Performance of Early Warning Indicators of Regime Shift. *Current biology*, **25**, 1867–1872.

Bestelmeyer BT, Ellison AM, Fraser WR et al. (2011) Analysis of abrupt transitions in ecological systems. *Ecosphere*, **2**, 129.

Bestelmeyer BT, Duniway MC, James DK, Burkett LM, Havstad KM (2013) A test of critical thresholds

bioRxiv preprint doi: https://doi.org/10.1101/091751; this version posted January 9, 2018. The copyright holder for this preprint (which was not certified by peer review) is the author/funder. All rights reserved. No reuse allowed without permission.

and their indicators in a desertification-prone ecosystem: more resilience than we thought. *Ecology Letters*, **16**, 339–345.

Boettiger C, Hastings A (2012) Quantifying limits to detection of early warning for critical transitions. *Journal of The Royal Society Interface*, **9**, 2527–2539.

Bonan GB (2008) Forests and Climate Change: Forcings, Feedbacks, and the Climate Benefits of Forests. *Science*, **320**, 1444–1449.

Botet R, Ploszajczak M (2004) Correlations in Finite Systems and Their Universal Scaling Properties. In: *Nonequilibrium physics at short time scales: Formation of correlations* (ed Morawetz K), pp. 445–466. Springer-Verlag, Berlin Heidelberg.

Brook BW, Ellis EC, Perring MP, Mackay AW, Blomqvist L (2013) Does the terrestrial biosphere have planetary tipping points? *Trends in Ecology & Evolution*.

Burnham K, Anderson DR (2002) Model selection and multi-model inference: A practical information-theoretic approach, 2nd. edn. Springer-Verlag, New York, pp.

Canfield DE, Glazer AN, Falkowski PG (2010) The Evolution and Future of Earth's Nitrogen Cycle. *Science*, **330**, 192–196.

Carpenter SR, Cole JJ, Pace ML et al. (2011) Early Warnings of Regime Shifts: A Whole-Ecosystem Experiment. *Science*, **332**, 1079–1082.

Clauset A, Shalizi C, Newman M (2009) Power-Law Distributions in Empirical Data. *SIAM Review*, **51**, 661–703.

Corrado R, Cherubini AM, Pennetta C (2014) Early warning signals of desertification transitions in semiarid ecosystems. *Physical Review E - Statistical, Nonlinear, and Soft Matter Physics*, **90**, 62705.

Crawley MJ (2012) The R Book, 2nd. edn. Wiley, Hoboken, NJ, USA, pp.

Crowther TW, Glick HB, Covey KR et al. (2015) Mapping tree density at a global scale. *Nature*, **525**, 201–205.

Dai L, Vorselen D, Korolev KS, Gore J (2012) Generic Indicators for Loss of Resilience Before a Tipping Point Leading to Population Collapse. *Science*, **336**, 1175–1177.

DiMiceli C, Carroll M, Sohlberg R, Huang C, Hansen M, Townshend J (2015) Annual Global Automated MODIS Vegetation Continuous Fields (MOD44B) at 250 m Spatial Resolution for Data Years Beginning

bioRxiv preprint doi: https://doi.org/10.1101/091751; this version posted January 9, 2018. The copyright holder for this preprint (which was not certified by peer review) is the author/funder. All rights reserved. No reuse allowed without permission.

Day 65, 2000 - 2014, Collection 051 Percent Tree Cover, University of Maryland, College Park, MD, USA.

Drake JM, Griffen BD (2010) Early warning signals of extinction in deteriorating environments. *Nature*, **467**, 456–459.

Efron B, Tibshirani RJ (1994) An Introduction to the Bootstrap. Taylor & Francis, New York, pp.

Filotas E, Parrott L, Burton PJ et al. (2014) Viewing forests through the lens of complex systems science. *Ecosphere*, **5**, 1–23.

Foley JA, Ramankutty N, Brauman KA et al. (2011) Solutions for a cultivated planet. *Nature*, **478**, 337–342.

Folke C, Jansson Å, Rockström J et al. (2011) Reconnecting to the Biosphere. *AMBIO*, **40**, 719–738.

Fung T, O'Dwyer JP, Rahman KA, Fletcher CD, Chisholm RA (2016) Reproducing static and dynamic biodiversity patterns in tropical forests: the critical role of environmental variance. *Ecology*, **97**, 1207–1217.

Gardner RH, Urban DL (2007) Neutral models for testing landscape hypotheses. *Landscape Ecology*, **22**, 15–29.

Gastner MT, Oborny B, Zimmermann DK, Pruessner G (2009) Transition from Connected to Fragmented Vegetation across an Environmental Gradient: Scaling Laws in Ecotone Geometry. *The American Naturalist*, **174**, E23–E39.

Gauthier S, Bernier P, Kuuluvainen T, Shvidenko AZ, Schepaschenko DG (2015) Boreal forest health and global change. *Science*, **349**, 819 LP–822.

Gilman SE, Urban MC, Tewksbury J, Gilchrist GW, Holt RD (2010) A framework for community interactions under climate change. *Trends in Ecology & Evolution*, **25**, 325–331.

Goldstein ML, Morris SA, Yen GG (2004) Problems with fitting to the power-law distribution. *The European Physical Journal B - Condensed Matter and Complex Systems*, **41**, 255–258.

Haddad NM, Brudvig La, Clobert J et al. (2015) Habitat fragmentation and its lasting impact on Earth's ecosystems. *Science Advances*, **1**, 1–9.

Hansen MC, Potapov PV, Moore R et al. (2013) High-Resolution Global Maps of 21st-Century Forest Cover Change. *Science*, **342**, 850–853.

Hansen M, Potapov P, Margono B, Stehman S, Turubanova S, Tyukavina A (2014) Response to Comment on "High-resolution global maps of 21st-century forest cover change". *Science*, **344**, 981.

Hantson S, Pueyo S, Chuvieco E (2015) Global fire size distribution is driven by human impact and climate.

bioRxiv preprint doi: https://doi.org/10.1101/091751; this version posted January 9, 2018. The copyright holder for this preprint (which was not certified by peer review) is the author/funder. All rights reserved. No reuse allowed without permission.

Global Ecology and Biogeography, **24**, 77–86.

Harris TE (1974) Contact interactions on a lattice. *The Annals of Probability*, **2**, 969–988.

Hartigan JA, Hartigan PM (1985) The Dip Test of Unimodality. *The Annals of Statistics*, **13**, 70–84.

Hastings A, Wysham DB (2010) Regime shifts in ecological systems can occur with no warning. *Ecology Letters*, **13**, 464–472.

He F, Hubbell S (2003) Percolation Theory for the Distribution and Abundance of Species. *Physical Review Letters*, **91**, 198103.

Heffernan JB, Soranno PA, Angilletta MJ et al. (2014) Macrosystems ecology: understanding ecological patterns and processes at continental scales. *Frontiers in Ecology and the Environment*, **12**, 5–14.

Hinrichsen H (2000) Non-equilibrium critical phenomena and phase transitions into absorbing states. *Advances in Physics*, **49**, 815–958.

Hirota M, Holmgren M, Nes EHV, Scheffer M (2011) Global Resilience of Tropical Forest and Savanna to Critical Transitions. *Science*, **334**, 232–235.

Irvine MA, Bull JC, Keeling MJ (2016) Aggregation dynamics explain vegetation patch-size distributions. *Theoretical Population Biology*, **108**, 70–74.

Keitt TH, Urban DL, Milne BT (1997) Detecting critical scales in fragmented landscapes. *Conservation Ecology*, **1**, 4.

Kéfi S, Rietkerk M, Alados CL, Pueyo Y, Papanastasis VP, ElAich A, Ruiter PC de (2007) Spatial vegetation patterns and imminent desertification in Mediterranean arid ecosystems. *Nature*, **449**, 213–217.

Kéfi S, Guttal V, Brock WA et al. (2014) Early Warning Signals of Ecological Transitions: Methods for Spatial Patterns. *PLoS ONE*, **9**, e92097.

Kitzberger T, Aráoz E, Gowda JH, Mermoz M, Morales JM (2012) Decreases in Fire Spread Probability with Forest Age Promotes Alternative Community States, Reduced Resilience to Climate Variability and Large Fire Regime Shifts. *Ecosystems*, **15**, 97–112.

Koenker R (2016) quantreg: Quantile Regression.

Lasco RD, Pulhin FB, Cruz RVO, Pulhin JM, Roy SSN, Sanchez PAJ (2008) Forest responses to changing rainfall in the Philippines. In: *Climate change and vulnerability* (eds Leary N, Conde C, Kulkarni J), pp.

bioRxiv preprint doi: https://doi.org/10.1101/091751; this version posted January 9, 2018. The copyright holder for this preprint (which was not certified by peer review) is the author/funder. All rights reserved. No reuse allowed without permission.

49–66. Earthscan, London.

Leibold MA, Norberg J (2004) Biodiversity in metacommunities: Plankton as complex adaptive systems? *Limnology and Oceanography*, **49**, 1278–1289.

Lenton TM, Williams HTP (2013) On the origin of planetary-scale tipping points. *Trends in Ecology & Evolution*, **28**, 380–382.

Lenton TM, Held H, Kriegler E, Hall JW, Lucht W, Rahmstorf S, Schellnhuber HJ (2008) Tipping elements in the Earth's climate system. *Proceedings of the National Academy of Sciences*, **105**, 1786–1793.

Limpert E, Stahel WA, Abbt M (2001) Log-normal Distributions across the Sciences: Keys and CluesOn the charms of statistics, and how mechanical models resembling gambling machines offer a link to a handy way to characterize log-normal distributions, which can provide deeper insight into var. *BioScience*, **51**, 341–352.

Loehle C, Li B-L, Sundell RC (1996) Forest spread and phase transitions at forest-praire ecotones in Kansas, U.S.A. *Landscape Ecology*, **11**, 225–235.

Malhi Y, Gardner TA, Goldsmith GR, Silman MR, Zelazowski P (2014) Tropical Forests in the Anthropocene. *Annual Review of Environment and Resources*, **39**, 125–159.

Manor A, Shnerb NM (2008) Origin of pareto-like spatial distributions in ecosystems. *Physical Review Letters*, **101**, 268104.

Martensen AC, Ribeiro MC, Banks-Leite C, Prado PI, Metzger JP (2012) Associations of Forest Cover, Fragment Area, and Connectivity with Neotropical Understory Bird Species Richness and Abundance. *Conservation Biology*, **26**, 1100–1111.

McKenzie D, Kennedy MC (2012) Power laws reveal phase transitions in landscape controls of fire regimes. *Nat Commun*, **3**, 726.

Mitchell MGE, Suarez-Castro AF, Martinez-Harms M et al. (2015) Reframing landscape fragmentation's effects on ecosystem services. *Trends in Ecology & Evolution*, **30**, 190–198.

Naito AT, Cairns DM (2015) Patterns of shrub expansion in Alaskan arctic river corridors suggest phase transition. *Ecology and Evolution*, **5**, 87–101.

Newman MEJ (2005) Power laws, Pareto distributions and Zipf's law. *Contemporary Physics*, **46**, 323–351.

Oborny B, Meszéna G, Szabó G (2005) Dynamics of Populations on the Verge of Extinction. *Oikos*, **109**,

bioRxiv preprint doi: https://doi.org/10.1101/091751; this version posted January 9, 2018. The copyright holder for this preprint (which was not certified by peer review) is the author/funder. All rights reserved. No reuse allowed without permission.

291–296.

Oborny B, Szabó G, Meszéna G (2007) Survival of species in patchy landscapes: percolation in space and time. In: *Scaling biodiversity*, pp. 409–440. Cambridge University Press.

Ochoa-Quintero JM, Gardner TA, Rosa I, de Barros Ferraz SF, Sutherland WJ (2015) Thresholds of species loss in Amazonian deforestation frontier landscapes. *Conservation Biology*, **29**, 440–451.

Ódor G (2004) Universality classes in nonequilibrium lattice systems. *Reviews of Modern Physics*, **76**, 663–724.

Pardini R, Bueno A de A, Gardner TA, Prado PI, Metzger JP (2010) Beyond the Fragmentation Threshold Hypothesis: Regime Shifts in Biodiversity Across Fragmented Landscapes. *PLoS ONE*, **5**, e13666.

Potapov P, Yaroshenko A, Turubanova S et al. (2008a) Mapping the world's intact forest landscapes by remote sensing. *Ecology and Society*, **13**.

Potapov P, Hansen MC, Stehman SV, Loveland TR, Pittman K (2008b) Combining MODIS and Landsat imagery to estimate and map boreal forest cover loss. *Remote Sensing of Environment*, **112**, 3708–3719.

Prishchepov AV, Müller D, Dubinin M, Baumann M, Radeloff VC (2013) Determinants of agricultural land abandonment in post-Soviet European Russia. *Land Use Policy*, **30**, 873–884.

Pueyo S, de Alencastro Graça PML, Barbosa RI, Cots R, Cardona E, Fearnside PM (2010) Testing for criticality in ecosystem dynamics: the case of Amazonian rainforest and savanna fire. *Ecology Letters*, **13**, 793–802.

R Core Team (2015) R: A Language and Environment for Statistical Computing.

Reyer CPO, Rammig A, Brouwers N, Langerwisch F (2015) Forest resilience, tipping points and global change processes. *Journal of Ecology*, **103**, 1–4.

Rockstrom J, Steffen W, Noone K et al. (2009) A safe operating space for humanity. *Nature*, **461**, 472–475.

Rooij MMJW van, Nash B, Rajaraman S, Holden JG (2013) A Fractal Approach to Dynamic Inference and Distribution Analysis. *Frontiers in Physiology*, **4**.

Rudel TK, Coomes OT, Moran E, Achard F, Angelsen A, Xu J, Lambin E (2005) Forest transitions: towards a global understanding of land use change. *Global Environmental Change*, **15**, 23–31.

Saravia LA, Momo FR (2017) Biodiversity collapse and early warning indicators in a spatial phase transition

bioRxiv preprint doi: https://doi.org/10.1101/091751; this version posted January 9, 2018. The copyright holder for this preprint (which was not certified by peer review) is the author/funder. All rights reserved. No reuse allowed without permission.

between neutral and niche communities. *PeerJ PrePrints*, **5**, e1589v4.

Scanlon TM, Caylor KK, Levin SA, Rodriguez-iturbe I (2007) Positive feedbacks promote power-law clustering of Kalahari vegetation. *Nature*, **449**, 209–212.

Scheffer M, Walkerk B, Carpenter S, Foley J a, Folke C, Walker B (2001) Catastrophic shifts in ecosystems. *Nature*, **413**, 591–596.

Scheffer M, Bascompte J, Brock WA et al. (2009) Early-warning signals for critical transitions. *Nature*, **461**, 53–59.

Seidler TG, Plotkin JB (2006) Seed Dispersal and Spatial Pattern in Tropical Trees. *PLoS Biology*, **4**, e344.

Sexton JO, Song X-P, Feng M et al. (2013) Global, 30-m resolution continuous fields of tree cover: Landsat-based rescaling of MODIS vegetation continuous fields with lidar-based estimates of error. *International Journal of Digital Earth*, **6**, 427–448.

Sexton JO, Noojipady P, Song X-P et al. (2015) Conservation policy and the measurement of forests. *Nature Climate Change*, **6**, 192–196.

Solé RV (2011) Phase Transitions. Princeton University Press, pp.

Solé RV, Bascompte J (2006) Self-organization in complex ecosystems. Princeton University Press, New Jersey, USA., pp.

Solé RV, Alonso D, Mckane A (2002) Self-organized instability in complex ecosystems. *Philosophical transactions of the Royal Society of London. Series B, Biological sciences*, **357**, 667–681.

Solé RV, Alonso D, Saldaña J (2004) Habitat fragmentation and biodiversity collapse in neutral communities. *Ecological Complexity*, **1**, 65–75.

Solé RV, Bartumeus F, Gamarra JGP (2005) Gap percolation in rainforests. *Oikos*, **110**, 177–185.

Staal A, Dekker SC, Xu C, Nes EH van (2016) Bistability, Spatial Interaction, and the Distribution of Tropical Forests and Savannas. *Ecosystems*, **19**, 1080–1091.

Stauffer D, Aharony A (1994) Introduction To Percolation Theory. Tayor & Francis, London, pp.

Vasilakopoulos P, Marshall CT (2015) Resilience and tipping points of an exploited fish population over six decades. *Global Change Biology*, **21**, 1834–1847.

Verbesselt J, Umlauf N, Hirota M et al. (2016) Remotely sensed resilience of tropical forests. *Nature Climate*

bioRxiv preprint doi: https://doi.org/10.1101/091751; this version posted January 9, 2018. The copyright holder for this preprint (which was not certified by peer review) is the author/funder. All rights reserved. No reuse allowed without permission.

Change, **1**.

Villa Martín P, Bonachela JA, Muñoz MA (2014) Quenched disorder forbids discontinuous transitions in nonequilibrium low-dimensional systems. *Physical Review E*, **89**, 12145.

Villa Martín P, Bonachela JA, Levin SA, Muñoz MA (2015) Eluding catastrophic shifts. *Proceedings of the National Academy of Sciences*, **112**, E1828–E1836.

Viña A, McConnell WJ, Yang H, Xu Z, Liu J (2016) Effects of conservation policy on China's forest recovery. *Science Advances*, **2**, e1500965.

Vuong QH (1989) Likelihood Ratio Tests for Model Selection and Non-Nested Hypotheses. *Econometrica*, **57**, 307–333.

Weerman EJ, Van Belzen J, Rietkerk M, Temmerman S, Kéfi S, Herman PMJ, Koppel JV de (2012) Changes in diatom patch-size distribution and degradation in a spatially self-organized intertidal mudflat ecosystem. *Ecology*, **93**, 608–618.

Weissmann H, Shnerb NM (2016) Predicting catastrophic shifts. *Journal of Theoretical Biology*, **397**, 128–134.

Wuyts B, Champneys AR, House JI (2017) Amazonian forest-savanna bistability and human impact. *Nature Communications*, **8**, 15519.

Xu C, Hantson S, Holmgren M, Nes EH van, Staal A, Scheffer M (2016) Remotely sensed canopy height reveals three pantropical ecosystem states. *Ecology*, **97**, 2518–2521.

Zhang JY, Wang Y, Zhao X, Xie G, Zhang T (2005) Grassland recovery by protection from grazing in a semi-arid sandy region of northern China. *New Zealand Journal of Agricultural Research*, **48**, 277–284.

Zinck RD, Grimm V (2009) Unifying wildfire models from ecology and statistical physics. *The American naturalist*, **174**, E170–85.